IEEE Access
Multidisciplinary | Rapid Review | Open Access Journal

Date of publication xxxx 00, 0000, date of current version xxxx 00, 0000.

Digital Object Identifier 10.1109/ACCESS.2023.0322000

Least Absolute Value Based Temperature-Dependent Robust State Estimation

YOHAN PARK[1], JEUK KANG[1], (Student Member, IEEE), GYEONG-HUN KIM[2], (Member, IEEE), and YUN-SU KIM[1], (Senior Member, IEEE)

[1]Graduate School of Energy Convergence, Gwangju Institute of Science and Technology (GIST), Gwangju 61005, Korea
[2]Smart Distribution Research Center, Korea Electrotechnology Research Institute (KERI), Changwon 51543, Korea

Corresponding author: Yun-Su Kim (e-mail: yunsukim@gist.ac.kr).

This research was supported by Korea Electrotechnology Research Institute (KERI) Primary research program through the National Research Council of Science & Technology (NST) funded by the Ministry of Science and ICT (MSIT) (No. 23A01022), and in part by the Korean Institute of Energy Technology Evaluation and Planning(KETEP) and the Ministry of Trade, Industry & Energy(MOTIE) of the Republic of Korea (No. 20225500000060).

ABSTRACT Inaccuracies in both measurements and parameter determination can generate biased results in state estimation. The change in branch temperature precipitates fluctuations in resistance and branch flow measurements. Even when flow measurements derived from remote terminal units are precise, the erroneous resistance value can still render the estimation results inaccurate. In this paper, we propose a least absolute value based, temperature-dependent, static state estimation method. The proposed method is formulated as a linear programming, employing an L1 norm objective function and introducing a branch temperature with the expanded Jacobian to consider thermal inertia. The proposed estimator not only estimates the state but also estimates branch temperature along with the resistance. Therefore, our proposed method captures the accurate system states robust against the parameter error and measurement error. Furthermore, the proposed estimator can evaluate thermal inertia with higher accuracy compared to the existing method. The case studies illustrate the robustness of the proposed method against parameter and measurement inaccuracies. Additionally, it can estimate state and thermal inertia more effectively than the comparative estimator.

INDEX TERMS Branch temperature, least absolute value, power system state estimation, thermal inertia.

A. INDEXES

k	index of bus k
ij	index of line from bus i to bus j

B. PARAMETERS

e	Measurement error vector
σ	Standard deviation vector of measurement
E	Covariance matrix of measurement
c	Vector of ones
ε	Residual threshold
γ	Iteration threshold
z	Measurement vector
P_{ij}	Measurement of active power flow at line ij
Q_{ij}	Measurement of reactive power flow at line ij
P_k	Measurement of active power injection at bus k
Q_k	Measurement of reactive power injection at bus k
R_θ	Thermal resistance
X_{ij}	Reactance at line ij
$T_{Ref,ij}$	Reference temperature at line ij
$T_{F,ij}$	Thermal constant at line ij

C. VARIABLES

x	State vector
t	Temperature vector
r	Residual vector
H_t	Jacobian matrix of measurement corresponding to state
H_t	Jacobian matrix of measurement corresponding to temperature
Δz	Linearized measurement vector
Δx	Linearized state vector
Δt	Linearized temeprature vector
N	Iteration index
T_{ij}	Temperature at line ij
V_k	Voltage magnitude at bus k
θ_k	Phase angle at bus k
S	Residual sensitivity matrix

I. INTRODUCTION

The function of power systems state estimation (SE) primarily lies in the consistent monitoring of system status. As the adoption of renewable energy sources keeps on rising rapidly, the importance of effectively monitoring power systems has been accentuated. In light of this trend, accurately determining the status of power systems has become indispensable for monitoring and control operations [1]. There have been relentless endeavors to enhance the performance of power systems state estimation. Notwithstanding these efforts, measurement and parameter errors persist as formidable barriers to accurate estimation. These errors often compromise the ability to provide a reliable solution for state estimators, leading to a challenging robustness problem [2].

In an attempt to mitigate this robustness issue, significant strides have been made toward the development of robust state estimators [3]–[5]. In [6], extended LAV (ELAV) which is robust against measurement and parameter error was proposed. In [7], ELAV which is robust against errors of control input for AC/DC grid is proposed. These algorithms are grounded on the principles of weighted least squares (WLS) and least absolute value (LAV). However, they provide a relatively elementary approach to identifying and adjusting outliers that amplify the value of the loss function. In [8], [9], estimators based on maximum correntropy were proposed which is robust against Gaussian noise and outliers. In [10], a maximum likelihood estimator based on Mahalanobis distance calculates the optimal phasor measurement units (PMU) buffer length. Nevertheless, these algorithms are devoid of any physically based guidance.

Branch temperature has been identified as a significant contributor to parameter error owing to its influence on branch resistance. A temperature-dependent power flow methodology that encompasses an estimation of branch temperatures and resistances has been proposed [11], [12]. By incorporating the thermal inertia of the conductor, the resistance can be rectified and consequently, more realistic power flow outcomes can be realized. In response to this, temperature-dependent weighted least squares (TDWLS) have been introduced [13]–[15]. However, these methods are fundamentally based on WLS, which inherently suffers from robustness shortcomings; they have not been compared with other state estimators. Given the inevitable presence of errors in measurements and parameters, coupled with the nonlinear nature of the system model, WLS estimators tend to minimize the residual of bad data, meaning that estimated values are fit to erroneous data. Consequently, the estimation outcomes of WLS estimators might not represent the optimal solution [2].

Conversely, LAV serves as a robust state estimator that rejects bad data by collecting measurements that have low residuals. Utilizing this methodology, a robust state estimator can be developed that uses sensibly corrected measurements, even in scenarios characterized by low redundancy [3], [6]. Power systems comprise a significant number of measurement errors and parameter errors. Over time, the precision of transmission branch parameters tends to deteriorate [2]. The LAV state estimator includes partial data, which closely approximate the truth values, in the base set. Employing these data with the base set can facilitate the attainment of robust estimation results.

In this paper, we propose a temperature-dependent least absolute value (TDLAV) method, a variant of the LAV approach, to develop a robust temperature-dependent state estimator. TDLAV takes into account thermal inertia by introducing a new variable, branch temperature, and expanding the Jacobian. This physically-guided approach to thermal inertia enables the estimation of not only the state but also the branch temperature, which depends on branch resistance. By factoring in branch temperature with an adjusted formulation, robust state estimation results can be derived from the linear programming (LP) solver. The contributions are outlined as follows:

1) Proposing a LAV-based robust state estimation algorithm to estimate the system state and branch temperature simultaneously with the novel formulation when the parameter error and measurement error exist.
2) The proposed state estimator displays resilience against the parameter error induced by changes in branch temperature. Furthermore, the $L1$ norm optimization of the LAV-based estimator corrects sensible measurement data and robustly estimates system states against the parameter error and measurement error.
3) The proposed estimator effectively estimates the state and thermal inertia of the branch. Compared to the existing method, the proposed TDLAV state estimation method demonstrates superior performance in estimating state and branch temperature.

The rest of this paper follows this structure: Section II introduces the preliminaries for the proposed method. Section III details the proposed TDLAV state estimation method. Section IV presents case studies employing the proposed method. Lastly, Section V concludes the paper.

II. PRELIMINARIES

A. CONVENTIONAL STATIC STATE ESTIMATION

Conventional state estimation algorithms seek to estimate states that minimize the objective function. The most frequently employed static state estimation techniques are WLS and LAV. The nonlinear measurement equation is as follows:

$$z = h(x) + e, \tag{1}$$

where x represents the state vector to be estimated, z denotes the measurement vector, e is the measurement error vector, and $h(\cdot)$ is the nonlinear function transforming x into z, equivalent to the measurement function.

The objective function of the WLS state estimation is defined as

$$\min_{x} \quad J(x) = c^T \| \frac{1}{\sigma^2} r \|_2^2, \tag{2}$$

where c is a vector of ones, r is a residual vector representing the difference of the measurement vector Δz and the

reconstructed measurement vector $\Delta\hat{z} = H_x\Delta\hat{x}$. The term σ denotes the standard deviation vector of the measurement error, whereas $J(\cdot)$ represents the objective function. Due to the $L2$ norm property of the residual vector, the objective function of the WLS state estimation is differentiable. Using the calculated differential of the objective function $\partial J/\partial x$, the initialized states are iteratively updated with the update term incorporating $\partial J/\partial x$ [16]. For Gaussian measurement errors, WLS state estimation delivers highly accurate results.

However, regarding leverage errors, WLS SE tends to yield biased results. Research into bad data detection and identification methods, such as [17], [18], has been conducted to address bias problems. Several robust SE techniques, including LAV, have been proposed to mitigate these issues. The LAV SE method can effectively identify a set of measurements less affected by measurement errors with the residual constraint. Consequently, it can exclude bad data and provide a robust estimation that remains uninfluenced by such erroneous data.

The objective function of LAV SE is defined as

$$\begin{aligned} \min \quad & c^T \|r\|_1 \\ \text{s.t.} \quad & \Delta z = H_x \Delta x + r, \end{aligned} \tag{3}$$

where r is the residual vector, H_x is the Jacobian matrix of (1) and Δx is the increment of state x used for updating. The objective of LAV SE is to determine Δx, which results in the minimized residual vector r. The $L1$ norm, which is not differentiable, is adopted for LAV SE. To minimize this $L1$ norm objective function, LAV SE is formulated as a LP problem. The formulation (3) is expressed as follows for implementation.

$$\begin{aligned} \min \quad & c^T (r^+ + r^-) \\ \text{s.t.} \quad & \Delta z = H_x \Delta x^+ - H_x \Delta x^- + r^+ - r^- \\ & \Delta x^+, \Delta x^-, r^+, r^- \geq 0, \end{aligned} \tag{4}$$

where the vectors r^+, r^-, Δx^+, and Δx^- are positive and negative parts of the residual and state, as follows:

$$r = r^+ - r^- \tag{5}$$

$$\Delta x = \Delta x^+ - \Delta x^-, \tag{6}$$

The difference of objective function between the WLS estimator and the LAV estimator is described in Fig. 1. This is the reason why the WLS and LAV estimators adopt the Gauss-Newton method and LP method respectively. Through the $L1$ norm objective function and residual constraint, the LAV estimator, contrary to the WLS estimator, effectively discards measurement error by correcting measurements with the residual constraint and minimizing the sum of the residual vector using LP solvers [6]. Also for the high residual as Fig. 1., the LAV estimator has a lower weight(derivative) than the WLS estimator which does not overestimate the high residual point and equally estimates the weight of residual. Hence, the LAV state estimator is robust against measurement error.

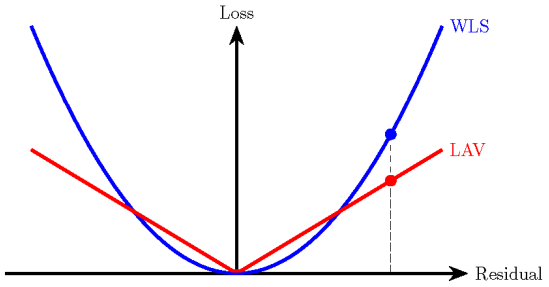

FIGURE 1. Objective function of WLS and LAV

B. TEMPERATURE DEPENDENT RESISTANCE

Line temperature varies in response to power loss, whereas resistance changes according to temperature. These variations can be depicted with respective equations. The resistance of metallic conductors, as outlined in [19], is given by

$$R = R_{\text{Ref}} \cdot \frac{T + T_{\text{F}}}{T_{\text{Ref}} + T_{\text{F}}}, \tag{7}$$

where R represents the conductor resistance, T denotes the conductor temperature, R_{Ref} is the conductor resistance at the reference temperature, T_{Ref} represents the reference temperature, and T_{F} is a temperature constant. The temperature constant T_{F} varies depending on the conductor metal: 234.5°C for copper and 228.1°C for hard-drawn aluminum [19], [20]. Additionally, the thermal resistance R_θ, the ratio of steady-state temperature rise to loss, is given by [20], defined as

$$\frac{T_{Rise}}{P_{Loss}} = \frac{T_{\text{RatedRise}}}{P_{\text{RatedLoss}}} = R_\theta, \tag{8}$$

where T_{Rise} indicates the device temperature rise above ambient temperature, $P_{\text{Loss}}(= I^2R)$ represents the total loss affecting temperature rise, T_{RefRise} is the reference device temperature rise, and R_{RefRise} is the reference loss. By combining equations (7) and (8), the generalized temperature model is derived [11] as follows:

$$T_{ij} = T_{\text{Amb}} + R_{\theta,ij} \cdot P_{\text{Loss},ij}, \tag{9}$$

$$P_{\text{Loss},ij} = G_{ij}(V_i^2 + V_j^2) - 2G_{ij} \cdot V_i V_j \cos\theta_{ij}, \tag{10}$$

where θ_{ij} refers to the difference in phase angle between θ_i and θ_j. G_{ij} represents the conductance computed from resistance and reactance. Consequently, according to (9) and (10), if T_{F}, T_{Amb} and R_θ are provided, the branch temperature can be calculated. The proportional relationship between power loss and temperature is depicted in Fig. 2. This temperature rise leads to a change in branch resistance and consequently causes deviations in the measurements from their values before the temperature increase. The impedance of a branch is sensitive to temperature fluctuations. Hence, the influence of temperature variation on line impedance must be taken into account. Consequently, the temperature-dependent power flow was proposed in [11], which integrates line temperature as a variable and computes the line temperature using voltage magnitude and phase angle.

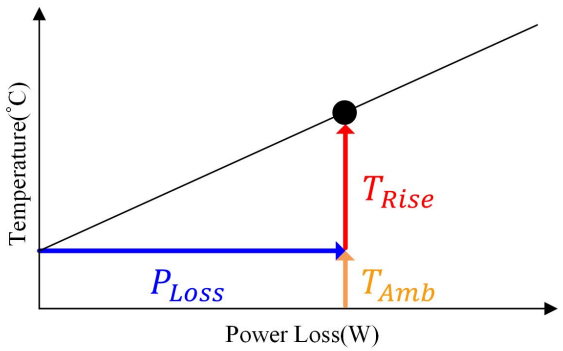

FIGURE 2. Conductor temperature according to power loss

C. LEVERAGE MEASUREMENT ERROR

The leverage measurement error is one of the main reasons for the inaccuracy of state estimators. This leverage point measurement can occur in situations such as below [2]:

1) A injection measurement point positioned at a bus that connects to numerous branches.
2) A injection measurement point positioned at a bus that connects to branches of significantly different impedance.
3) A flow measurement along branches with impedances significantly divergent from those of the others.
4) Using an exceedingly huge weight for a particular measurement.

Shortly, leverage point measurements have much bigger weights than the others. The non-interacting measurement error and the interacting measurement error are sort of leverage measurement error [21], [22]. The updating term of the WLS estimator is below:

$$\begin{aligned}\Delta x &= (H^T E^{-1} H)^{-1} H^T E^{-1} \Delta z \\ &= G^{-1} H^T E^{-1} \Delta z, \end{aligned} \tag{11}$$

where E is the covariance matrix of measurement and $G = H^T E^{-1} H$. The residual sensitivity matrix is as follows:

$$S = (I - H G^{-1} H^T E^{-1}), \tag{12}$$

The residual sensitive matrix characterizes non-interacting measurement error and interacting measurement error [23]. If $S_{ik} \approx 0$, it is said to be non-interacting for measurements i and k. In this case, the normalized residual test can identify the erroneous data. If S_{ik} is significantly large, the measurements i and k are interacting. In contrast to the non-interacting error, there are measurements in which the normalized residual test fails: interacting conforming error. The measurement in which the normalized residual test works is called interacting non-conforming error.

III. PROPOSED METHOD

A. MEASUREMENT EQUATION

The estimation of states employs measurements assumed to be acquired from remote terminal units, such as branch active power flow P_{ij} and branch reactive power flow Q_{ij}. Additionally, the branch temperature mismatch M_{ij}, a new measure for power flow introduced in [11], is adopted for the LAV state estimation. The branch temperature mismatch M_{ij} is a vector consisting solely of zeros; it is a defined, not an acquired, measurement, thereby eliminating the need for additional measurements. By minimizing the $L1$ norm residual of the temperature mismatch M_{ij}, the proposed estimator accurately estimates the initialized states x and t. The temperature mismatch M_{ij} converges to zero upon updating the states. The measurement equation for each measurement follows the approach presented in [11]:

$$P_{ij}(V,\theta,T) = V_i^2 - V_i V_j G_{ij} \cos\theta_{ij} - V_i V_j B_{ij} \sin\theta_{ij}, \tag{13}$$

$$\begin{aligned} Q_{ij}(V,\theta,T) = &-V_i V_j G_{ij} \sin\theta_{ij} - V_i^2 B_{ij} \\ &+ V_i V_j B_{ij} \cos\theta_{ij}, \end{aligned} \tag{14}$$

$$\begin{aligned} M_{ij}(V,\theta,T) = T_{ij} - (T_{Amb} + R_{\theta,ij}(G_{ij}(V_i^2 + V_j^2) \\ -2G_{ij} V_i V_j \cos\theta_{ij})) = 0, \end{aligned} \tag{15}$$

where G_{ij} and B_{ij} are conductance and susceptance calculated with the temperature-dependent resistance (7) as below:

$$G_{ij} = \frac{R_{ij}}{R_{ij}^2 + X_{ij}^2}, \tag{16}$$

$$B_{ij} = \frac{X_{ij}}{R_{ij}^2 + X_{ij}^2}, \tag{17}$$

where X_{ij} is the branch reactance. The differential terms of conductance and susceptance for constructing the Jacobian matrix are as follows:

$$\frac{\partial R_{ij}}{\partial T_{ij}} = \frac{R_{Ref,ij}}{T_{Ref,ij} + T_{F,ij}}, \tag{18}$$

$$\frac{\partial G_{ij}}{\partial T_{ij}} = \frac{X_{ij}^2 - R_{ij}^2}{R_{ij}^2 + X_{ij}^2} \cdot \frac{R_{Ref,ij}}{T_{Ref,ij} + T_{F,ij}}, \tag{19}$$

$$\frac{\partial B_{ij}}{\partial T_{ij}} = \frac{2X_{ij}R_{ij}}{R_{ij}^2 + X_{ij}^2} \cdot \frac{R_{Ref,ij}}{T_{Ref,ij} + T_{F,ij}} \tag{20}$$

B. PROBLEM FORMULATION

For the estimation of temperature-dependent states, the TD-LAV state estimation is formulated as follows:

$$\begin{aligned} \min \quad & \|r\|_1 + \|D\Delta t\|_1 \\ \text{s.t.} \quad & \Delta z = H_x \Delta x + H_t \Delta t + r, \end{aligned} \tag{21}$$

where the state vector x comprises node phase angles θ_i and node voltage magnitudes V_i. The newly introduced state branch temperature t consists of T_{ij}, which is a branch temperature from node i to node j initialized by (9). Furthermore, $H_t = {}^{\partial H}/_{\partial t}$ represents the Jacobian matrix corresponding to temperature.

In [6], this scaling vector was adopted for scaling the parameter vector which enables the estimation of differently scaled variables. The TDLAV also incorporates the normalizing vector D. The vector D comprises elements d_i, where d_i is

1 divided by the mean of the i^{th} row of H_t. For the proposed TDLAV, normalization is required because the branch temperature values have different scales compared to the residuals. This normalization method is Lasso regularization which is widely adopted to state estimation [24]–[26]. Through Lasso regularization, the branch temperature can be estimated adequately.

The proposed formulation is expressed as an LP problem:

$$\begin{aligned} \min \quad & c^T(r^+ + r^-) + D^T(\Delta t^+ + \Delta t^-) \\ \text{s.t.} \quad & \Delta z = H_x\Delta x^+ - H_x\Delta x^- + H_t\Delta t^+ - H_t\Delta t^- + r^+ - r^- \\ & \Delta x^+, \Delta x^-, \Delta t^+, \Delta t^-, r^+, r^- \geq 0, \end{aligned} \tag{22}$$

where r and Δx are the same as in (5) and (6). The newly introduced variables Δt^+ and Δt^- are defined as follows:

$$\Delta t = \Delta t^+ - \Delta t^-, \tag{23}$$

The Jacobian matrices H_x and H_t, which correspond to state and temperature respectively, are defined as

$$H_x = \begin{bmatrix} \partial P/\partial\theta & \partial P/\partial V \\ \partial Q/\partial\theta & \partial Q/\partial V \\ \partial M/\partial\theta & \partial M/\partial V \end{bmatrix}, \tag{24}$$

$$H_t = \begin{bmatrix} \partial P/\partial T \\ \partial Q/\partial T \\ \partial M/\partial T \end{bmatrix}, \tag{25}$$

C. SOLUTION STEPS

The proposed method estimates voltage magnitude, phase angle, and branch temperature by incorporating updating terms derived from the $L1$ norm state estimator in each iteration. The resistance is updated with the estimated temperature using the updated branch temperature obtained from (7) in every iteration. The units adopted are per unit (p.u.) for the voltage magnitude, with the voltage level of each bus serving as the base, radians (rad.) for the phase angle, Celsius for the branch temperature, and ohm for the resistance. The states are initialized as ''flat start'' with voltage magnitude set as 1.0 p.u. and voltage phase angle as 0 for all buses. The temperature is initialized as 25°C for all lines. The solution steps for TDLAV are described in Algorithm 1.

Algorithm 1 TDLAV

1: **Data** : measurement $z \ni \{P_{ij}, Q_{ij}, P_k, Q_k\}$
2: **Results** : state $x \ni \{V_k, \theta_k\}$, temperature $t \ni \{T_{ij}\}$
3: Initialize state x, temperature t;
4: **while** $\max r > \varepsilon \wedge N < \gamma$ **do**
5: Compute the linearized measurement vector;
6: $\Delta z \leftarrow z - h(x)$
7: Compute H_x, H_t;
8: Solve the LP problem by (22) and derive $\Delta x, \Delta t, r$;
9: Update state and temperature;
10: $x \leftarrow x + \Delta x$
11: $t \leftarrow t + \Delta t$
12: Update line resistance by (7);
13: Report x, t and line resistance;

IV. CASE STUDIES

For the assessment of the proposed method, we implemented TDLAV using the Python programming language; it was simulated on the 33-node test feeder and 118-node test feeder. The proposed TDLAV is compared with the WLS, LAV, weighted least absolute value (WLAV), iteratively reweighted least squares(IRLS), and TDWLS methods. The estimator WLAV and IRLS are the reformulated state estimators from the LAV that are weighted with the measurement vector and residual vector respectively [27], [28]. These estimators are robust against the measurement error. For the measurements, active power flow P_{ij}, reactive power flow Q_{ij}, active power injection P_k, and reactive power injection Q_k are used to estimate system state voltage magnitude V_k, voltage phase angle θ_k and branch temperature T_{ij}. In the case of a 33-node test feeder, the numbers of each measurement and estimating variables are 32, 32, 33, 33, 33, 33, and 32 concerning P_{ij}, Q_{ij}, P_k, Q_k, V_k, θ_k, and T_{ij}. In the case of a 118-node test feeder, the numbers of each measurement and estimating variables are 173, 173, 118, 118, 118, 118, and 173 concerning P_{ij}, Q_{ij}, P_k, Q_k, V_k, θ_k, and T_{ij}. Consequently, for the 33-node test feeder, the redundancy, the ratio of the measurement and estimating variables, is 1.32 for the TDWLS and TDLAV and 1.96 for the other estimators. In the meanwhile, for the 118-node test feeder, the redundancy is 1.42 for the TDWLS and TDLAV and 2.46 for the other estimators.

The proposed TDLAV is assessed under three scenarios: 1) the presence of Gaussian measurement noise along with changes in branch temperature and resistance; 2) the inclusion of Gaussian measurement noise and interacting leverage measurement error along with changes in branch temperature and resistance; 3) the inclusion of Gaussian measurement noise and non-interacting leverage measurement error along with changes in branch temperature and resistance. The Gaussian measurement noise is assumed as zero mean and is introduced within the 5% limit. The interacting leverage errors are imposed on randomly sampled measurements, amounting to up to 25%. The non-interacting leverage errors are imposed on randomly sampled measurements, missing the value and remaining zero. The branch temperature change is set as a rise of from 0°C to 10°C for all branches. For rational analysis, 1000 simulations were performed and compared for each scenario. In each simulation, the measurement errors and temperature variations are randomly imposed. The voltage estimation results of each estimator are compared with a target, which is the power flow result computed with the correct resistance and non-erroneous measurements should be estimated by each algorithm.

The accuracy of estimated values is evaluated as the mean absolute error (MAE) for the voltage magnitude, voltage phase angle, branch resistance, and branch temperature, for-

mulated as follows:

$$MAE = \frac{1}{n}\sum_{i=1}^{n}|x_i - \hat{x}_i|, \tag{26}$$

where n denotes the number of values, x_i the actual value, and $\hat{x}_i$ the estimated value. Additionally, another equation total vector error (TVE) is employed to assess the phasor voltage without separating it into magnitude and phase angle, defined as follows:

$$TVE = \sqrt{\frac{(Re(X) - Re(\hat{X}))^2 + (Im(X) - Im(\hat{X}))^2}{Re(X)^2 + Im(X)^2}}, \tag{27}$$

where X represents the complex actual value, $\hat{X}$ represents the complex estimated value, $Re(\cdot)$ denotes the real part, and $Im(\cdot)$ represents the imaginary part. The TVE is appropriate for phasor value evaluation by considering the amplitude and phase differences together [29].

The assumptions, for the implementation of TDLAV, are as below:

1) Target test feeders are balanced networks
2) Thermal constant $T_{F,ij}$ is equivalent for all lines as 228.1 °C (copper)
3) Inducing Gaussian measurement error within 5% limit for all measurements
4) For leverage measurement error scenarios, leverage error occurs for 10% of the total measurements

A. SCENARIO 1: GAUSSIAN NOISE AND TEMPERATURE CHANGE

In Scenario 1, the performance of the SE algorithms is evaluated under a branch temperature increase of from 0°C to 10°C along with the resistance and the measurements containing Gaussian noise. This scenario encounters common random errors in measurement devices during regular operations. For the 33 test feeder, the estimated voltage magnitude, voltage phase angle, and branch temperature are depicted in Fig. 3, Fig. 4, and Table 1. The results of a single simulation for node voltages and temperatures were depicted in Fig. 3a, Fig. 3b, and Fig. 4a. The MAE distribution results of the whole simulation are depicted in Fig. 3c, Fig. 3d, Fig. 4b, and Fig. 4c. In table 1, the average TVE and MAE of each algorithm's estimation result are described. The results indicate that the proposed TDLAV displays the lowest error for the estimated voltage, temperature, and resistance among the algorithms in the case of the 33 test feeder. In the meanwhile, the TDWLS shows the highest error for TVE of voltage estimation, MAE of temperature estimation, and MAE of resistance estimation.

For the 118 test feeder, the estimated voltage magnitude, voltage phase angle, and branch temperature are depicted in Fig. 5, Fig. 6, and Table 2. Unlike the 33 test feeder, the voltage magnitude estimation MAE of TDLAV was higher than LAV, WLAV, and IRLS. However, in terms of the phase angle estimation MAE, TDLAV shows the lowest error among the estimators. Therefore, the TDLAV has the lowest TVE, representing the error of phasor voltage. Also, like the 33-node test feeder, the TDLAV shows lower MAE about temperature estimation results. In contrast to the TDLAV estimator, the TDWLS estimator has the second-highest error for voltage estimation and the higher error for temperature and resistance estimation.

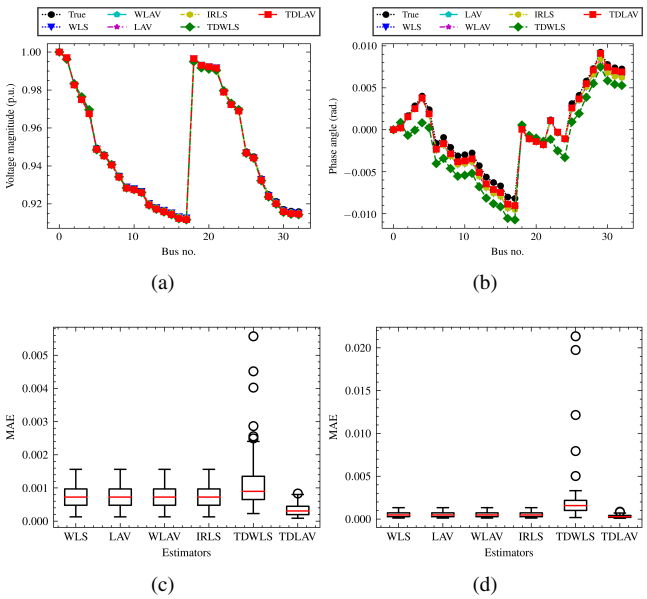

FIGURE 3. Scenario 1: 33-node test feeder. (a) voltage magnitudes, (b) phase angles, (c) MAE distribution of voltage magnitudes, (d) MAE distribution of phase angles.

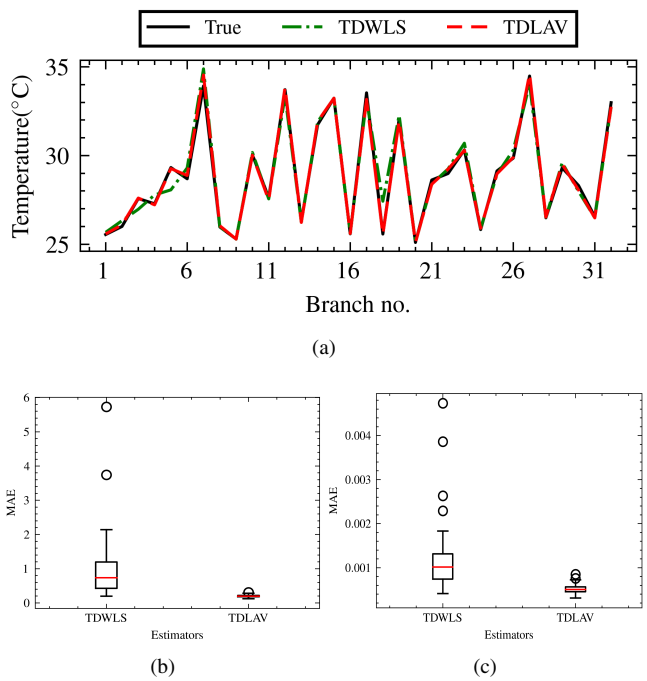

FIGURE 4. Scenario 1: 33-node test feeder. (a) branch temperature, (b) MAE distribution of branch temperature, (c) MAE distribution of resistance.

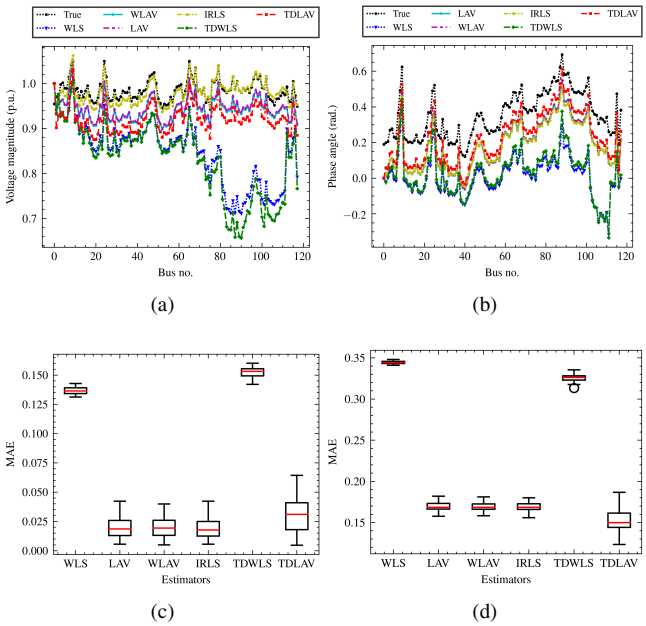

FIGURE 5. Scenario 1: 118-node test feeder. (a) voltage magnitudes, (b) phase angles, (c) MAE distribution of voltage magnitudes, (d) MAE distribution of phase angles.

TABLE 1. Estimation Performances for Scenario 1 : 33-node test feeder

Method	TVE	MAE			
	$\tilde{V}$	V(p.u.)	θ(rad.)	T(°C)	$R(\Omega)$
WLS	0.001032	0.000728	0.000530	-	-
LAV	0.001032	0.000728	0.000530	-	-
WLAV	0.001032	0.000728	0.000530	-	-
IRLS	0.001032	0.000728	0.000530	-	-
TDWLS	0.002635	0.001138	0.002132	0.874343	0.001134
TDLAV	0.000548	0.000343	0.000337	0.200964	0.000518

TABLE 2. Estimation Performances for Scenario 1 : 118-node test feeder

Method	TVE	MAE			
	$\tilde{V}$	V(p.u.)	θ(rad.)	T(°C)	$R(\Omega)$
WLS	0.346099	0.136645	0.344348	-	-
LAV	0.169553	0.020217	0.169585	-	-
WLAV	0.169227	0.020466	0.169271	-	-
IRLS	0.169144	0.019869	0.169150	-	-
TDWLS	0.335435	0.152609	0.325569	1.819309	0.297398
TDLAV	0.155450	0.030824	0.153086	0.497642	0.023998

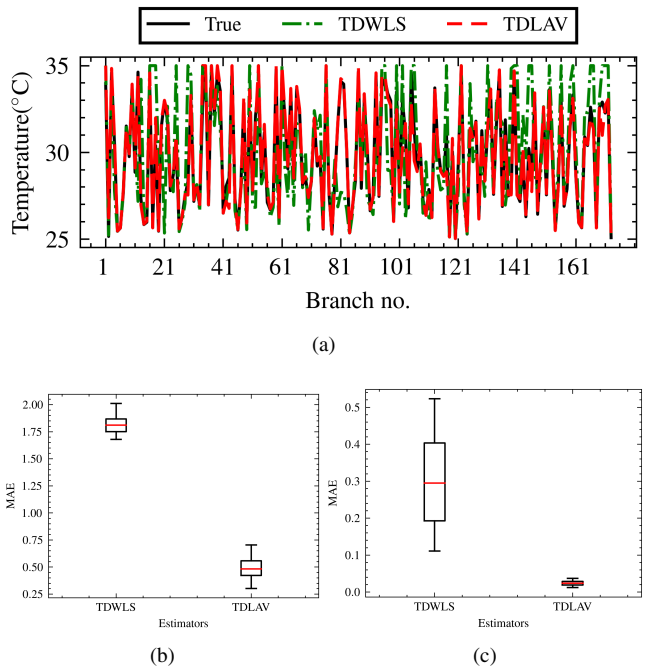

FIGURE 6. Scenario 1: 118-node test feeder. (a) branch temperature, (b) MAE distribution of branch temperature, (c) MAE distribution of resistance.

B. SCENARIO 2: GAUSSIAN NOISE, TEMPERATURE CHANGE, AND INTERACTING LEVERAGE ERROR

In Scenario 2, the performance of the SE algorithms is evaluated under Gaussian measurement noise, branch temperature increase from 0°C to 10°C, and interacting leverage error. The interacting leverage error is imposed within 25% for the randomly sampled 10% injection measurement and 10% flow measurement. This scenario encounters notable outliers within the set of measurements. These exceptional values simulate instances of equipment malfunction or data manipulation. The estimation results for the 33 test feeder are presented in Fig. 7, Fig. 8, and Table 3. The simulation results of node voltages and temperatures for a single case were depicted in Fig. 7a, Fig. 7b, and Fig. 8a. The MAE distribution results for whole cases are depicted in Fig. 7c, Fig. 7d, Fig. 8b, and Fig. 8c. The TDLAV shows the lowest TVE and MAE for the voltage estimation among the estimators. Also, the MAE for the temperature and resistance was lower than TDWLS. Compared to scenario 1, due to the interacting leverage error, the overall estimation error was higher.

For the 118 test feeder, estimation results are depicted in Fig. 9, Fig. 10, and Table 4. The TDLAV estimator shows the lowest TVE for phasor voltage estimation. It's due to the lowest MAE of phase angle estimation, even though it has a higher MAE for the voltage magnitude estimation. In the meantime, the TDWLS estimator has the second-highest TVE for the phasor voltage estimation beside the WLS estimator. The proposed TDLAV estimator significantly surpasses the other algorithms in terms of the TVE for the phasor voltage and MAE for temperature and resistance. The discrepancy in performance arises from the difference in the accuracy of branch temperature estimation, with TDWLS showing a lesser degree of accuracy than TDLAV which demonstrates a lower average MAE. The proposed TDLAV not only estimates the branch temperature more accurately but also more precisely determines the voltage estimation by incorporating Jacobian terms differentiated for branch temperature, which

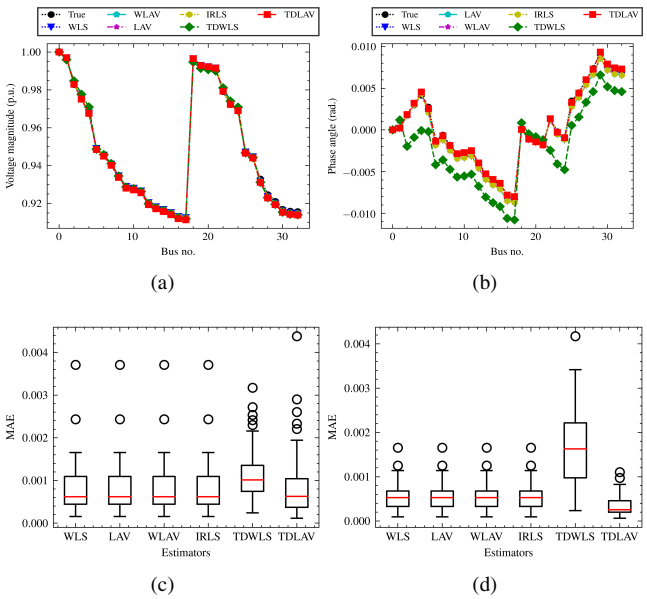

FIGURE 7. Scenario 2: 33-node test feeder. (a) voltage magnitudes, (b) phase angles, (c) MAE distribution of voltage magnitudes, (d) MAE distribution of phase angles.

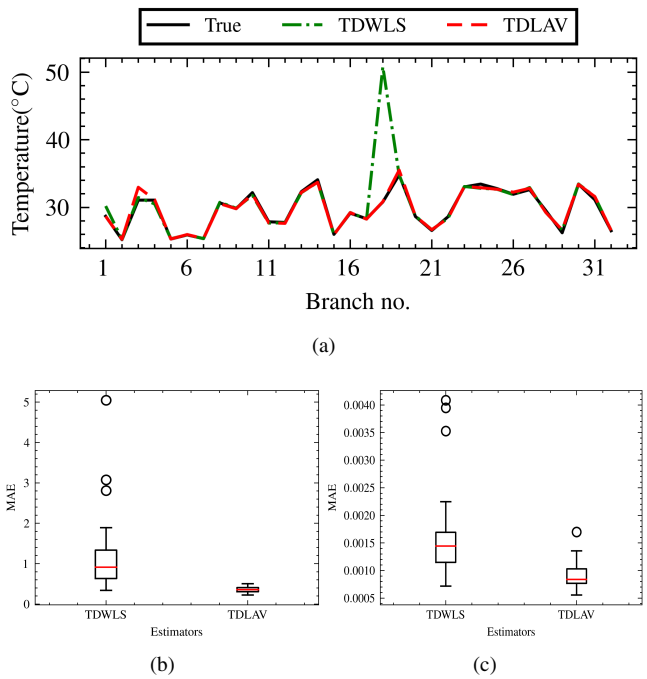

FIGURE 8. Scenario 2: 33-node test feeder. (a) branch temperature, (b) MAE distribution of branch temperature, (c) MAE distribution of resistance.

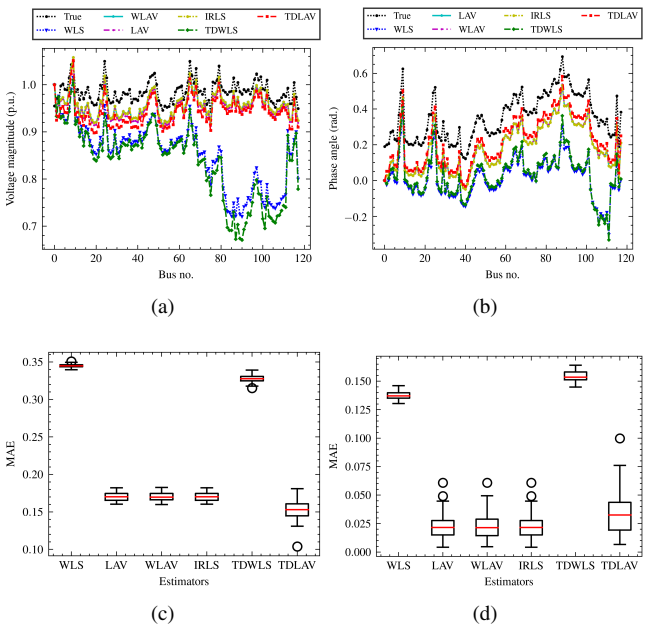

FIGURE 9. Scenario 2: 118-node test feeder. (a) voltage magnitudes, (b) phase angles, (c) MAE distribution of voltage magnitudes, (d) MAE distribution of phase angles.

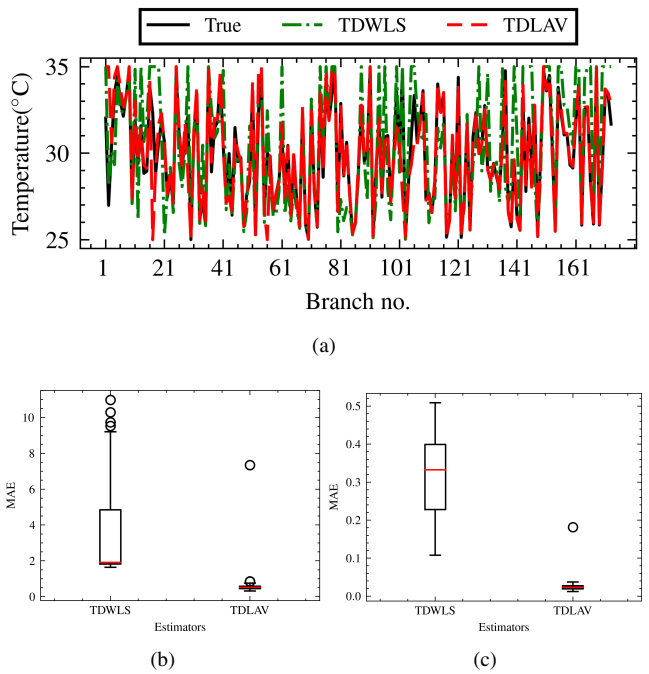

FIGURE 10. Scenario 2: 118-node test feeder. (a) branch temperature, (b) MAE distribution of branch temperature, (c) MAE distribution of resistance.

minimizes temperature mismatch.

C. SCENARIO 3: GAUSSIAN NOISE, TEMPERATURE CHANGE, AND NON-INTERACTING LEVERAGE ERROR

In Scenario 3, the estimation results are evaluated under Gaussian measurement noise, non-interacting measurement error, and branch temperature change. The branch temperature increases from 0°C to 10°C for all branches. The non-interacting measurement error is assumed to be zero value. This scenario reflects the cyber attack and malfunction of the equipment. These values cause highly biased estimation results. By replacing the value as zero, the weight becomes huge which causes the off-diagonal values of the residual

TABLE 3. Estimation Performances for Scenario 2 : 33-node test feeder

Method	TVE	MAE			
	$\tilde{V}$	V(p.u.)	θ(rad.)	T(°C)	$R(\Omega)$
WLS	0.001144	0.000804	0.000574	-	-
LAV	0.001144	0.000804	0.000574	-	-
WLAV	0.001144	0.000804	0.000574	-	-
IRLS	0.001144	0.000804	0.000574	-	-
TDWLS	0.003066	0.001177	0.001614	1.115052	0.001547
TDLAV	0.001102	0.000889	0.000343	0.358698	0.000894

TABLE 4. Estimation Performances for Scenario 2 : 118-node test feeder

Method	TVE	MAE			
	$\tilde{V}$	V(p.u.)	θ(rad.)	T(°C)	$R(\Omega)$
WLS	0.346752	0.137500	0.344903	-	-
LAV	0.170122	0.021871	0.170089	-	-
WLAV	0.170472	0.022568	0.170387	-	-
IRLS	0.170122	0.021871	0.170089	-	-
TDWLS	0.337326	0.154001	0.327496	3.398266	0.313847
TDLAV	0.155464	0.033995	0.152318	0.619079	0.025694

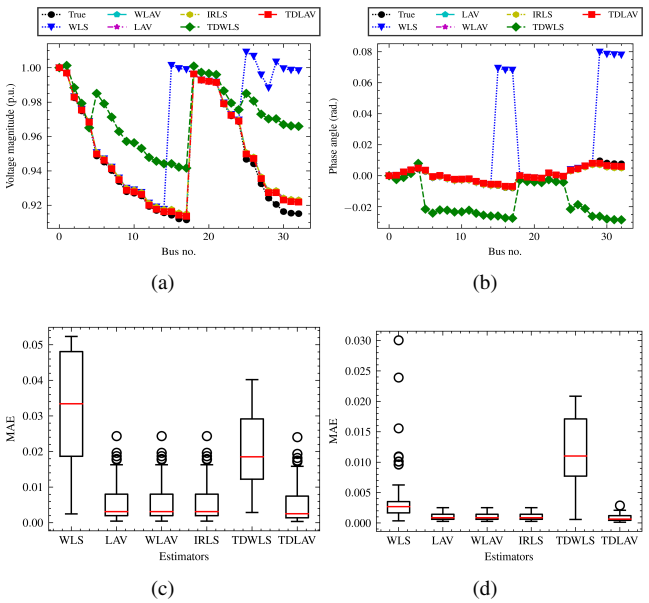

FIGURE 11. Scenario 3: 33-node test feeder. (a) voltage magnitudes, (b) phase angles, (c) MAE distribution of voltage magnitudes, (d) MAE distribution of phase angles.

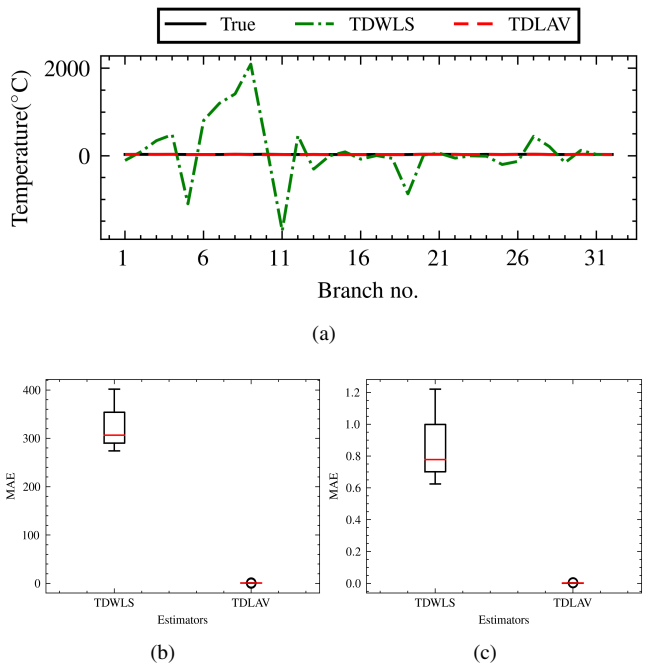

FIGURE 12. Scenario 3: 33-node test feeder. (a) branch temperature, (c) MAE distribution of branch temperature, (d) MAE distribution of resistance.

sensitivity matrix to be zero. The simulation results for the 33 test feeder are depicted in Fig. 11, Fig. 12, and Table 5. The comparative benchmarks are the same as those used in Scenario 1. and Scenario 2. Also, the results of a single simulation are depicted in Fig. 11a, Fig. 11b, and Fig. 12a. MAE distribution results for whole simulations are depicted in Fig. 11c, Fig. 11d, Fig. 12b, and Fig. 12c.

For the 33 test feeder, the TDLAV estimator shows the lowest error for all criteria such as TVE of phasor voltage, MAE of voltage magnitude, MAE of phase angle, MAE of temperature, and MAE of resistance. In the meanwhile, the TDWLS estimator shows the highest error for TVE of phasor voltage, MAE of temperature, and MAE of resistance. It's due to a non-interacting measurement error which causes the non-diagonal components of the residual sensitivity matrix to be zero. This error induces more biased estimation results than the other scenarios. For the 118 test feeder, the TDLAV shows the lowest error for the TVE of phasor voltage, MAE of phase angle, MAE of temperature, and MAE of resistance as shown in Fig. 13, Fig. 14, and Table. 14b. The TDWLS shows the second-highest error for the TVE of phasor voltage, MAE of temperature, and MAE of resistance. It also happened that non-interacting measurements caused biased estimation results. Compared to the 33 test feeder case, the redundancy is relatively high which helps the TDWLS estimator show lower error. In Scenario 3, the lack of robustness problem was most clearly described for the WLS estimator and TDWLS estimator.

For all scenarios, the proposed TDLAV estimator demonstrates superior performance over the other algorithms in terms of TVE for the phasor voltage, MAE for temperature, and MAE for resistance. Among the algorithms, TDLAV not only exhibits superior accuracy in branch temperature and resistance estimation but also estimates precise node voltage estimation. In the case of TDWLS, the branch temperature presents a higher error, which aligns with the findings of all scenarios. The superiority for overall estimation results demonstrated by the $L1$ norm-based TDLAV can be attributed

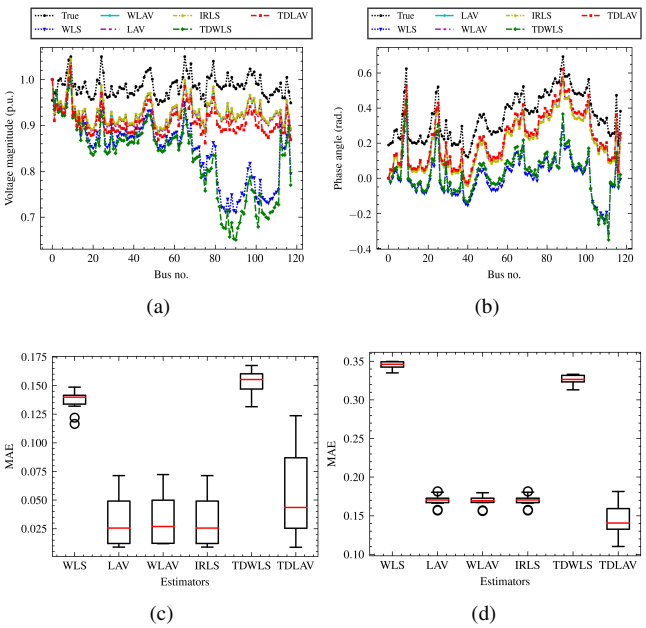

FIGURE 13. Scenario 3: 118-node test feeder. (a) voltage magnitudes, (b) phase angles, (c) MAE distribution of voltage magnitudes, (d) MAE distribution of phase angles.

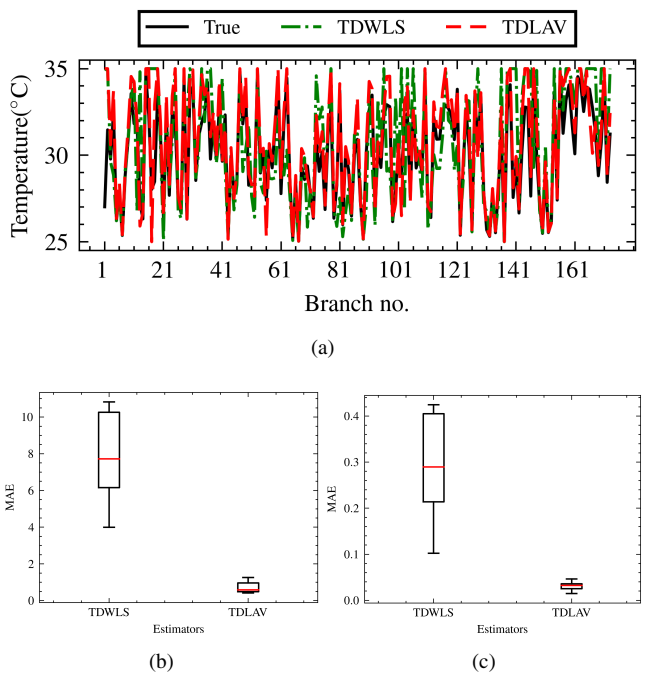

FIGURE 14. Scenario 3: 118-node test feeder. (a) branch temperature, (b) MAE distribution of branch temperature, (c) MAE distribution of resistance.

to the LP problem solver's robustness by sensible measurements correcting [6]. In contrast, TDWLS demonstrates the estimation results that are fit to erroneous measurements and parameters without sensible selection of given data. Furthermore, the TDLAV estimator shows the lowest TVE for phasor voltage for all scenarios. This means the TDLAV has

TABLE 5. Estimation Performances for Scenario 3 : 33-node test feeder

Method	TVE	MAE			
	$\tilde{V}$	V(p.u.)	θ(rad.)	T(°C)	$R(\Omega)$
WLS	0.038949	0.035331	0.003834	-	-
LAV	0.006234	0.005588	0.001027	-	-
WLAV	0.006234	0.005588	0.001027	-	-
IRLS	0.006234	0.005588	0.001027	-	-
TDWLS	0.112002	0.013655	0.008111	327.403161	0.874247
TDLAV	0.005681	0.005114	0.000891	0.661708	0.001744

TABLE 6. Estimation Performances for Scenario 3 : 118-node test feeder

Method	TVE	MAE			
	$\tilde{V}$	V(p.u.)	θ(rad.)	T(°C)	$R(\Omega)$
WLS	0.346633	0.136554	0.345028	-	-
LAV	0.172314	0.033334	0.169736	-	-
WLAV	0.171754	0.034335	0.169057	-	-
IRLS	0.172314	0.033334	0.169736	-	-
TDWLS	0.335628	0.152463	0.325945	7.955575	0.293881
TDLAV	0.158859	0.054105	0.145531	0.714185	0.031325

superior performance even compared to conventional robust state estimators like WLAV and IRLS.

Hence, the proposed TDLAV exhibits higher accuracy and robustness than conventional SE algorithms. The simulation results for each of the three scenarios, involving Gaussian noise, interacting leverage error, non-interacting leverage error, and temperature change, consistently indicate superior performance by the proposed approach over the traditional WLS, LAV, WLAV, IRLS, and TDWLS in terms of static state estimation. The major distinction from TDWLS is that TDLAV has the ability to correct measurements, providing accurate estimation results with a sensible set. This property enables TDLAV to produce more robust estimation results, whereas the comparative estimator TDWLS, which minimizes residuals for all measurements, generates biased values.

A dilemma, lack of robustness which WLS-based state estimators suffer, causes the inaccuracy of the TDWLS estimator. The error in measurements induces biased estimation results. In this regard, similar to the WLS estimator, the TDWLS estimator has a high estimation error. Furthermore, the TDWLS and TDLAV have lower redundancy (1.32 for the 33 test feeder and 1.42 for the 118 test feeder) than the other estimators (1.96 for the 33 test feeder and 2.46 for the 118 test feeder) because the estimating variables are expanded to temperature. According to [30], the variance of estimations can increase when redundancy decreases. Due to this lack of robustness and low redundancy, for the 33 test feeder, the TDWLS not only has the biggest error but also has the biggest variance of MAE in terms of voltage, temperature, and resistance in Scenario 1 and Scenario 2. In Scenario 3 with non-interacting leverage error, even though the TDWLS

has a lower variance than the WLS, it still exhibits a higher variance of MAE than the other estimators. However, for the 118 test feeder, the TDLAV has a higher variance of MAE in terms of voltage estimation in Scenario 1 and Scenario 2 as the redundancy of each estimator increases. Nevertheless, the TDLAV has the lowest average TVE of voltage estimation for all scenarios and test feeders by correcting sensible measurements with the residual constraint from the given measurement set [6].

For better estimator development, the thermal constant, which is assumed in this paper, should be rationally determined. The thermal constant can be identified with data-driven methods like [31], [32]. Identification of thermal constant dynamics will lead to the enhancement of thermal inertia assessment. Another issue, for the breakthrough, is measuring the temperature. The proposed method estimates state and temperature with the flow and injection measurement correlated to temperature. However, temperature measurements are required for advanced research and assessment. Temperature measurements can be collected through a Fiber Bragg Grating sensor likewise [33], [34]. Also, by thermal image, line temperature can be collected [35].

V. CONCLUSION

In this study, we proposed a LAV based temperature-dependent robust state estimation methodology. The formulation of LAV was extended to create TDLAV, which includes branch temperature. TDLAV takes into account changes in branch temperature in conjunction with resistance and flow measurements. The results estimated by TDLAV show reduced errors in comparison to other estimators. The proposed method offers enhanced levels of observability and more accurate system models by conducting robust estimation against measurement and parameter errors due to temperature variation. This research lays the groundwork for SE and opens avenues for extension into various systems. Future work can involve assessing thermal dynamics, different topologies, and actual systems.

ACKNOWLEDGMENT

This research was funded by the Korea Electrotechnology Research Institute (KERI) Primary research program through the National Research Council of Science & Technology (NST), which is supported by the Ministry of Science and ICT (MSIT) (Grant No. 23A01022). Partial funding was also provided by the Korean Institute of Energy Technology Evaluation and Planning (KETEP) and the Ministry of Trade, Industry & Energy (MOTIE) of the Republic of Korea (Grant No. 20225500000060).

REFERENCES

[1] G. Rietveld, J.-P. Braun, R. Martin, P. Wright, W. Heins, N. Ell, P. Clarkson, and N. Zisky, "Measurement infrastructure to support the reliable operation of smart electrical grids," *IEEE Trans. Instrum. Meas.*, vol. 64, no. 6, pp. 1355–1363, 2015.

[2] B. Gou and D. Shue, "Advances in algorithms for power system static state estimators: An improved solution for bad data management and state estimator convergence," *IEEE Power and Energy Magazine*, vol. 21, no. 1, pp. 16–25, 2023.

[3] M. Göl and A. Abur, "Lav based robust state estimation for systems measured by pmus," *IEEE Trans. Smart Grid*, vol. 5, no. 4, pp. 1808–1814, 2014.

[4] M. Allam and M. Laughton, "A general algorithm for estimating power system variables and network parameters," in *Proc. IEEE PES 1974 Summer Meeting*, 1974, pp. 331–5.

[5] M. S. Shahriar and I. O. Habiballah, "Hybridization of wls and lmr: a robust solution for power system state estimation," in *IEEE Sustainable Power and Energy Conference (iSPEC)*, 2022, pp. pp. 1–5.

[6] Y. Lin and A. Abur, "Robust state estimation against measurement and network parameter errors," *IEEE Trans. Power Syst.*, vol. 33, no. 5, pp. 4751–4759, 2018.

[7] Z. Fang, Y. Lin, S. Song, C. Li, X. Lin, F. Wang, and Y. Lu, "A comprehensive framework for robust ac/dc grid state estimation against measurement and control input errors," *IEEE Transactions on Power Systems*, vol. 37, no. 2, pp. 1067–1077, 2022.

[8] T. Chen, H. Ren, G. Chen, H. B. Gooi, and G. A. J. Amaratunga, "A distributed robust system-wide state estimation method for power systems based on maximum correntropy," *IEEE Transactions on Industrial Informatics*, vol. 19, no. 12, pp. 11 455–11 465, 2023.

[9] Y. Boukili, M. M. Ayiad, H. Moayyed, A. P. Aguiar, and Z. Vale, "Robust state estimation model for low voltage distribution networks in the presence of multiple gross errors," *IEEE Access*, vol. 11, pp. 42 403–42 415, 2023.

[10] H. Zhang, Q. Xu, Y. Xie, X. Lin, R. Ding, Y. Liu, C. Qiu, and P. Chen, "Robust state estimation method based on mahalanobis distance under non-gauss noise," *IEEE Access*, vol. 12, pp. 9243–9250, 2024.

[11] S. Frank, J. Sexauer, and S. Mohagheghi, "Temperature-dependent power flow," *IEEE Trans. Power Syst.*, vol. 28, no. 4, pp. 4007–4018, 2013.

[12] B. Ngoko, H. Sugihara, and T. Funaki, "A temperature dependent power flow model considering overhead transmission line conductor thermal inertia characteristics," in *2019 IEEE International Conference on Environment and Electrical Engineering and 2019 IEEE Industrial and Commercial Power Syst. Europe (EEEIC/I&CPS Europe)*, 2019, pp. 1–6.

[13] M. Wydra, "Performance and accuracy investigation of the two-step algorithm for power system state and line temperature estimation," *Energies*, vol. 11, no. 4, p. 1005, 2018.

[14] M. Bockarjova and G. Andersson, "Transmission line conductor temperature impact on state estimation accuracy," in *2007 IEEE Lausanne Power Tech*, 2007, pp. 701–706.

[15] M. Wydra and P. Kacejko, "Power system state estimation using wire temperature measurements for model accuracy enhancement," in *2016 IEEE PES Innovative Smart Grid Technologies Conference Europe (ISGT-Europe)*, 2016, pp. 1–6.

[16] H. Wang and N. Schulz, "A revised branch current-based distribution system state estimation algorithm and meter placement impact," *IEEE Trans. Power Syst.*, vol. 19, no. 1, pp. 207–213, 2004.

[17] E. Handschin, F. Schweppe, J. Kohlas, and A. Fiechter, "Bad data analysis for power system state estimation," *IEEE Trans. Power Apparatus and Systems*, vol. 94, no. 2, pp. 329–337, 1975.

[18] V. Quintana, A. Simoes-Costa, and M. Mier, "Bad data detection and identification techniques using estimation orthogonal methods," *IEEE Trans. Power Apparatus and Systems*, vol. PAS-101, no. 9, pp. 3356–3364, 1982.

[19] "Ieee standard test code for dry-type distribution and power transformers," *IEEE Std C57.12.91-2011 (Revision of IEEE Std C57.12.91-2001)*, pp. 1–94, 2012.

[20] "Ieee recommended practice for industrial and commercial power syst. analysis (brown book)," *IEEE Std 399-1997*, pp. 1–488, 1998.

[21] A. S. Dobakhshari, V. Terzija, and S. Azizi, "Normalized deleted residual test for identifying interacting bad data in power system state estimation," *IEEE Trans. Power Syst.*, vol. 37, no. 5, pp. 4006–4016, 2022.

[22] E. Asada, A. Garcia, and R. Romero, "Identifying multiple interacting bad data in power system state estimation," in *IEEE Power Engineering Society General Meeting*, 2005, pp. 571–577 Vol. 1.

[23] A. Abur and A. Expósito, *Power System State Estimation: Theory and Implementation*. CRC Press, 2004.

[24] Y. Liao, Y. Weng, and R. Rajagopal, "Urban distribution grid topology reconstruction via lasso," in *2016 IEEE Power and Energy Society General Meeting (PESGM)*, 2016, pp. 1–5.

[25] R. Gao, S. Särkkä, R. Claveria-Vega, and S. Godsill, "Autonomous tracking and state estimation with generalized group lasso," *IEEE Trans. Cybernetics*, vol. 52, no. 11, pp. 12 056–12 070, 2022.

[26] D. Duan, L. Yang, and L. L. Scharf, "Phasor state estimation from pmu measurements with bad data," in *2011 4th IEEE International Workshop on Computational Advances in Multi-Sensor Adaptive Processing (CAMSAP)*, 2011, pp. 121–124.
[27] A. Abur and M. Celik, "A fast algorithm for the weighted least absolute value state estimation (for power systems)," *IEEE Trans. Power Syst.*, vol. 6, no. 1, pp. 1–8, 1991.
[28] R. Pires, A. Simoes Costa, and L. Mili, "Iteratively reweighted least-squares state estimation through givens rotations," *IEEE Trans. Power Syst.*, vol. 14, no. 4, pp. 1499–1507, 1999.
[29] "Ieee/iec international standard - measuring relays and protection equipment - part 118-1: Synchrophasor for power systems - measurements," *IEC/IEEE 60255-118-1:2018*, pp. 1–78, 2018.
[30] P. J. Rousseeuw and A. M. Leroy, *Robust regression and outlier detection*. John wiley & sons, 2005.
[31] Y. Yang, R. G. Harley, D. Divan, and T. G. Habetler, "Overhead conductor thermal dynamics identification by using echo state networks," in *2009 International Joint Conference on Neural Networks*, 2009, pp. 3436–3443.
[32] D. L. Alvarez, F. F. da Silva, E. E. Mombello, C. L. Bak, and J. A. Rosero, "Conductor temperature estimation and prediction at thermal transient state in dynamic line rating application," *IEEE Trans. Power Del.*, vol. 33, no. 5, pp. 2236–2245, 2018.
[33] R. Chintakindi and S. P. S. Rajesh, "Vital role of fbg sensors — 2012 developments in electrical power systems," in *2013 International Conference on Power, Energy and Control (ICPEC)*, 2013, pp. 478–483.
[34] F. Barón, G. Álvarez Botero, F. Amortegui, D. Pastor, and M. Varón, "Temperature measurements on overhead lines using fiber bragg grating sensors," in *2017 IEEE International Instrumentation and Measurement Technology Conference (I2MTC)*, 2017, pp. 1–4.
[35] J. Wang and X. Zhang, "Electrical fault detection based on infrared temperature measurement technology," in *2023 IEEE 12th International Conference on Communication Systems and Network Technologies (CSNT)*, 2023, pp. 309–313.

YOHAN PARK completed his B.S. degree in electronic engineering at Chonnam National University, Gwangju, South Korea, in 2021. He is currently pursuing his Ph.D. degree at the Graduate School of Energy Convergence at Gwangju Institute of Science and Technology (GIST), Gwangju, Korea. His research focus is on distribution networks, distributed energy resources, and distribution network state estimation.

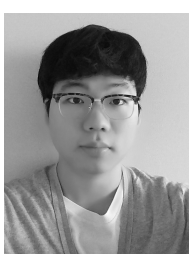

JEUK KANG graduated with a B.S. degree in electronic engineering from Hanyang University, Ansan, South Korea, in 2019. He is currently working toward his Ph.D. degree at the Graduate School of Energy Convergence at Gwangju Institute of Science and Technology (GIST), Gwangju, South Korea. His research interests include distribution networks, distributed energy resources, dynamic state estimation, grid identification, and optimal planning.

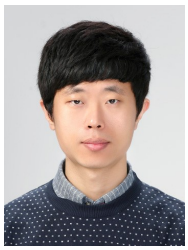

GYEONG-HUN KIM obtained his B.S., M.S., and Ph.D. degrees in Electrical Engineering from Changwon National University, Korea, in 2007, 2009, and 2013, respectively. Since 2013, he has been with the Korea Electrotechnology Research Institute (KERI), Changwon, Korea, where he currently holds the position of senior research engineer at the Smart Distribution Research Center. His research primarily focuses on the operation and control of power systems.

YUN-SU KIM received his B.S. and Ph.D. degrees in electrical engineering from Seoul National University, Seoul, South Korea, in 2010 and 2016, respectively. He served as a senior researcher at the Korea Electrotechnology Research Institute (KERI) from 2015 to 2017. In 2018, he joined the faculty of the Gwangju Institute of Science and Technology (GIST), where he is now an Associate Professor at the Graduate School of Energy Convergence. He served as the Director of the Korean Society for New and Renewable Energy and the Korean Institute of Electrical Engineers. His research areas include distribution networks, distributed energy resources, microgrids, artificial intelligence, and wireless power transfer.